Int J Adv Manuf Technol (2017) 91:2895–2906
DOI 10.1007/s00170-016-9960-y

ORIGINAL ARTICLE

Sintering of 17-4PH stainless steel powder assisted by microwave and the gradient of mechanical properties in the sintered body

J. Shi[1,2,3] · Z. Cheng[2] · J.C. Gelin[3] · T. Barriere[3] · B. Liu[2]

Received: 1 August 2016 / Accepted: 22 December 2016 / Published online: 12 January 2017

Abstract The sintering of 17-4PH stainless steel powder using microwaves has rarely been reported with results better than those produced by sintering with conventional resistive heating. This study evaluates the effect of the sintering temperature, holding time, heating rate and the pre-sintering stage in microwave-assisted sintering. By optimizing the sintering step to determine the optimal process, a more homogeneous microstructure, a greater sintered density, a greater shrinkage and better mechanical properties were obtained using microwave-assisted sintering. The total process time of the microwave-assisted sintering was notably less than conventional sintering, and the peak temperature was 150 to 200 °C lower. In 17-4PH stainless steel powder, microwave-assisted sintering was demonstrated to produce significantly better mechanical properties than conventional sintering. Measurements of the hardness distribution within the sintered specimen described the gradient of the mechanical properties of the microwave-sintered components. This study highlights why PM 17-4PH stainless steels should be produced using microwave-assisted sintering.

Keywords Microwave-assisted sintering · Powder injection moulding · Heating rate · Gradient in mechanical properties · 17-4PH

✉ T. Barriere
thierry.barriere@univ-fcomte.fr

[1] School of Civil Engineering and Architecture, Southwest University of Science and Technology, Mianyang 621010, China

[2] School of Mechanics and Engineering, Southwest Jiaotong University, Chengdu 610031, China

[3] UBFC, Department of Applied Mechanics, Femto-ST Institute, Besançon, 24 Rue de l'Epitaphe, 25030 Besançon, France

1 Introduction

17-4PH stainless steel is a type of martensitic precipitation-hardened material with high-performance mechanical properties [1]. Via heat treatment, high yield strengths of up to 1300 MPa can be achieved. With its excellent corrosion resistance, this versatile material is widely used in the aerospace, chemical, petrochemical, food processing, nuclear and general metalworking industries. Most studies related to the sintering of 17-4PH stainless steel have investigated conventional resistive heating (CRH); for example, Ye et al. [2] investigated the densification behaviour of this material at 650–1050 °C. Sung et al. investigated the effect of sintering kinetics by tensile testing micropowder injection moulding (PIM) 17-4PH specimens and specifically tested the influence of the cooling stage on the microstructural, tensile and fatigue properties. The results were compared with conventionally produced 17-4PH products [3]. The combination of 17-4PH stainless steel powder with a rubber binder provides increased mechanical properties of the sintered specimens. The optimal heating rate of 5 °C/min during sintering results in a greater density, greater tensile strength, less porosity and a more homogenous grain shape morphology [4].

17-4PH powders have been used in powder injection moulding, which is a type of the powder metallurgy, to create fully dense or porous components with functional properties. For example, Mutlu and Oktay [5] successfully used the space holder technique and CRH sintering to produce highly porous 17-4PH stainless steel with porosities between 39 and 82%. Suri et al. [6] performed Charpy V-notch impact tests on full-sized and small specimens to describe the impact properties of sintered and wrought 17-4PH stainless steel. Simchi et al. [7] experimented with a bilayer structure and discovered that the strain rate of 17-4PH was greater than 316L during sintering. Imgrund et al. [8] also produced magnetic-non-magnetic bimetals made from

316L/17-4PH and 316L/Fe powders using micrometal injection moulding and the CRH sintering process.

Microwave (MW) heating results from the absorption of the energy transported from an oscillating electromagnetic field [9]. This absorption manifests as molecular vibrations (i.e., rotating electric dipole/dipole reorientations) and ionic conduction in the sintered materials. The absorbed energy is transformed into heat, which sinters the powdered material. At low temperatures, the metal powder exhibits poor coupling with the microwaves [10]. The MW-assisted sintering is a process in which the sintered material absorbs the electromagnetic energy from microwaves. The furnaces that are typically used for MW-assisted sintering operate at a frequency of 2.45 GHz, while the reported tests were measured at greater than 8.0 GHz. The primary advantages of MW-assisted sintering are detailed as follows: rapid densification kinetics, reducing the required time and energy, rapid internal heating [11], lower peak temperature [12], finer microstructures and improved mechanical properties [13]. To apply MW-assisted sintering, many studies investigated different powder materials. Chockalingam et al. have investigated the phase transformation, microstructure and mechanical properties of two MW-assisted sintering materials: silicon nitride (Si_3N_4) with lithium yttrium oxide ($LiYO_2$) and zirconia (ZrO_2) sintering additives [14] and β-SiAlON-ZrO_2 composites [15]. Bykov et al. [16] investigated the influence of MW heating on mass transport phenomena and phase transformations in nanostructured ceramic materials. Chandrasekaran et al. [17] conducted MW heating and melting of lead, tin, aluminium and copper with a silicon carbide susceptor. Srinath et al. [18] illustrated a novel method to join bulk metallic materials with high thermal conductivities, such as copper, using MW heating. Panda et al. [19] compared the effect of the heating mode on the densification, microstructure, strength and hardness of austenitic (316L) and ferritic (434 L) stainless steels. The advantages of MW-assisted sintering were all confirmed in these studies.

For the magnetic induction of sintered powder in microwave heating, not all the metallic materials interact with the magnetic fields. The non-ferrous metals, as well as some stainless steels in austenitic structures, are not inducible to magnetics. However, 17-4PH stainless steel is a magnetic inducible material. Only one study that investigated the MW processing of 17-4PH stainless steel powder was found in the literature. That study was a preliminary investigation performed by Bose et al. [20], and the results indicated that MW-assisted sintering did not improve the mechanical properties of the 17-4PH stainless steel compared to CRH sintering. Thus, more research must be performed regarding the properties of 17-4PH stainless steel using MW-assisted sintering.

In common practice, the MW sinterability of a material is determined from many factors; the dominant factors are the sintering process' parameters, which include the sintering temperature, the holding time, the heating rate and the pre-sintering stage [21]. The sintering atmosphere also has an important impact on the corrosion behaviour and mechanical properties of the resulting material. Stainless steel powders should be sintered in hydrogen or argon atmospheres with low dew points or in a vacuum to reduce oxidation [22]. The particle size of the powder is also an important factor; powders with smaller particles produce denser materials with higher performance mechanical properties [23]. Some recent studies using compact 316L stainless samples have illustrated the effects of the heating rate used in microwave-assisted sintering on the densification, tensile strength and elongation of the sintered results [24]. The use of finer stainless steel powders improves the physical and mechanical properties of the samples sintered using both methods [24].

The authors established a complete frame of simulation for MW-assisted sintering using COMSOL software that included heat generation in the powder due to the microwaves and the densification of the sintered components [25]. This simulation frame was built using test data: the multi-physics modelling and simulation of MW heating [26], the simulation of the heat transfer in the sintered body and the sintering behaviours described in a previous study [27]. The constitutive law for sintering stainless steel powders could be integrated using COMSOL through the User subroutine; however, this subroutine does not consider the electromagnetic properties of stainless steel powders at different temperatures or at different relative densities. The measurement of the complex permittivity and permeability on magnetic stainless steel powder is also required within the filler of the MW absorber composite. This measurement, however, does not accurately describe the MW-assisted sintering of nearly pure stainless steel powder after debinding [28]. A measurement was taken based on barium and strontium ferrite powders, but the frequency used was markedly greater than the frequency used in the furnace for MW-assisted sintering [29].

To better understand the sintering properties of 17-4PH stainless steel, this study examined the densification and the microstructure evolution of 17-4PH stainless steel powder produced using MW-assisted sintering. The injected specimens were subjected to 2.45 GHz microwaves in a multi-mode furnace, and the effects of different processing factors during sintering were investigated. After solid-state sintering, the evolution of the microstructure, the densification and the mechanical response of sintered specimens were studied by analysing the Vickers hardness and ultimate tensile stress. A comparison of materials produced using MW-assisted sintering and the CRH process was also performed.

2 Experimental procedure

2.1 Materials

The experimental specimens were made of water-atomized commercial AISI 17-4PH stainless steel powder with an average particle size of 11 μm. The water-atomized particles had

irregular shapes. The chemical composition of the 17-4PH stainless steel used in this study is shown in Table 1 and was based on standard AISI630.

2.2 Process description of debinding and sintering stages

In this study, the green portions of the 17-4PH stainless steel powders were prepared via several processes before MW-assisted sintering. The stainless steel powders were first mixed with wax-based thermoplastic binders based on the appropriate polymer–powder formulations that were optimized by Kong et al. [30] and were then formed with injection moulding equipment. The density of the green portions was approximately 5.05 g/cm^3, which was 64% of the density of pure 17-4PH stainless steel (7.89 g/cm^3).

The binder in the injected specimen was almost completely removed during the two debinding stages using sequential solvent and thermal methods [31, 32]. Before sintering, binders were debound in an argon atmosphere to prevent oxidation. An electric thermal debinding oven was used. The first stage was to remove the water vapour held within the powder. The injected components were thus heated from 20 to 130 °C at a heating rate 55 °C/h; this temperature is lower than the decomposition temperature of the paraffin wax. Then, the temperature was increased up to 220 °C at a slower heating rate of 4.5 °C/h to remove the paraffin wax. The specimens were then cooled for 2 h to the ambient temperature. This debinding cycle was also used by Quinard et al. [31] when studying PIM feedstock with 316L stainless steel powder (mean particle size = 3.4 μm) to investigate the microcomponents. In powder metallurgy, finer starting powder particles are known to have better sinterability and, therefore, tend to achieve relatively greater sintered densities. During the debinding process, the weight of the specimens was reduced by 6.3%. This preliminary debinding stage was necessary to prevent cracking in the next sintering stage [32].

The research of Quinard et al. [31], who investigated the CRH sintering of 316L stainless steel, was used as a reference for the experimental set-up used in this study. The heating processes included three steps. First, the specimens were heated to 600 °C and held at that temperature for 30 min to completely remove the remaining binder components. Then, the temperature was increased to 900 °C and held again for 30 min. Finally, the temperature was increased to the peak value of the prescribed test and then held again for 10 min. It was expected that during the heating process, the residual binder would continue to decompose, leading to a decrease in weight. The weight gain during sintering with an increase in the temperature implied that some reactions in addition to the decomposition of the residual binder had occurred during sintering.

The schematic illustration of all of the steps (i.e., from powder particles to sintered parts) is shown in Fig. 1. The experiments in this paper show that the pre-sintered specimens of the compacted 17-4PH stainless steel powder possess the necessary initial stiffness for the beginning of the sintering process. The final sintering stage is represented by two possible methods: CRH or MW-assisted sintering.

A high-temperature microwave laboratory system (HAMilab-V1500, 2.45 GHz) was used in this study, based on a multi-mode microwave cavity. The continuously adjustable microwave power varied from 0.2 to 1.35 kW. The maximum working temperature was 1600 °C, and the maximum heating rate could exceed 50 °C/min. The surface temperature of the specimen was continuously measured using a high accuracy Raytek IR pyrometer from an exterior cavity window. The IR sensor detects the temperature from 600 to 1600 °C, and the temperature accuracy is approximately ±0.5%. The precision of the measurement is subject to many factors, including the sample size and its surface quality, the emissivity according to the material composition, the sample IR pyrometer alignment, the variation of emissivity with temperature, etc. The pyrometer measures the radiant energy from the sample surface and determines the temperature based on a preset emissivity. The temperature measurements for all the compacted powder specimens were made based on the preset emissivity of steel (0.35) [33]. The MW heating behaviour of metal powder compact is influenced by a few factors, including the design of the MW cavity, the physic properties of the materials, the number of samples and their position in the cavity, etc. A flat SiC was placed under the compacted powder, and certain chopped susceptors were placed around the powder based on the research by Kim-Hak et al. [34].

To study the densification behaviour at different heating modes, the same debound components were also sintered using CRH in a vertical SETSYS® SETARAM evolution analyser. The dilatometer sintering CRH tests, in an analyser, have been performed in a primary vacuum of approximately 10^{-3} mbar. The MW-assisted sintering tests were performed in argon atmosphere due to the atmosphere control of the microwave laboratory system.

Table 1 Chemical composition of 17-4PH stainless steel (wt%)

Fe	Ni	Cr	C	Cu	Nb	Mn	S	P	Si
71.8–73.8	3.0–3.5	15.5–17.5	≤0.07	3.0–5.0	0.45	≤1.0	≤0.03	≤0.04	≤1.0

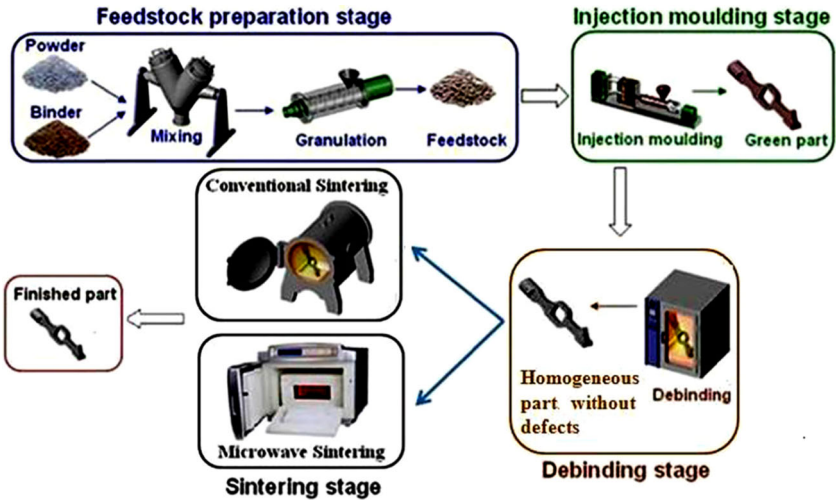

Fig. 1 Sequential stages to obtain the final sintered parts. The sintering stage can be processed using the CRH or MW methods

2.3 Sizes of the specimens after being injected, debound and undergoing MW-assisted sintering

The sizes of the specimens after being injected, debound and undergoing MW-assisted sintering were measured and compared, as shown in Fig. 2, and exhibit marked shrinkages after sintering (e.g., approximately 15% along the *x*-direction).

2.4 Material characterization of the sintered specimens

To evaluate the results of the sintering process, certain measurements and observations were performed and analysed. The shrinkage of the sintered specimens was measured using callipers, and the bulk densities of the specimens were tested using Archimedes' principle. For the measurements, the samples were immersed into an ethanol-based liquid; then, two sets of sintered samples that had been sintered under the same sintering conditions were wet-polished using a manual polisher. One set was used to measure the hardness distribution in the sintered body; the polished section was in the middle plane of the sintered component with nearly half of the body removed. The other set was used to observe and analyse the material's microstructures; the polished section was near the exterior surface, and only a thin layer of the sintered material was removed to expose and prepare this section. The distribution of the Vickers bulk hardness in the middle section of the sintered body was measured at nine locations arranged equidistantly along two perpendicular directions (i.e., *x* and *y*). The measurements were performed using a 5-kg load and a 10-s duration. To obtain reliable measurements, the hardness at each location was recorded as the average of five readings near the location on the prepared section of the middle plane.

For clear observations, the observed areas of the specimens were polished and chemically etched. Metallographic processes were used in the microstructural analyses, and a 4% nitric acid solution and alcohol were used to etch the polished surface. Next, an optical microscope was used to observe the microstructure of the polished and chemically etched specimen surfaces.

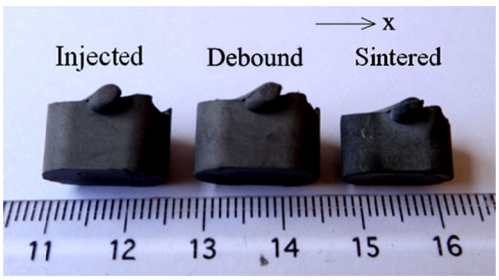

Fig. 2 Size comparison after injection moulding, thermal debinding and MW-assisted sintering of 17-4PH stainless steel powder specimens

3 Results and discussion

3.1 Important factors in the MW-assisted sintering process

3.1.1 Peak sintering temperature

The optimal peak temperature of the MW-assisted sintering of the 17-4PH stainless steel powder is expected to be less than the peak temperature of CRH sintering. To determine the effect of the peak temperature on the sintering results, tests were performed at different peak temperatures, while other processing factors remained the same. Therefore, any variation in the results was affected only by the change in the peak temperature. The debinding and pre-sintering kinetics have been described in paragraph 1.2. The same heating rate of 5 °C/min was used, and the specimen was held at the peak temperature for 10 min in all test processes, and the results produced by the different peak temperatures are shown in Table 2.

Table 2 shows that a suitable peak temperature will result in optimized results. For the MW-assisted sintering of the 17-

Table 2 Comparison of the shrinkages along the *x*-direction (shown in Fig. 2), the relative densities and the Vickers hardnesses

Peak temperature (°C)	Size shrinkage (%)	Relative density (%)	Vickers hardness (HV)
1100	5.67 ± 0.5	72.6 ± 0.11	173 ± 3
1140	10.29 ± 0.4	90.5 ± 0.06	280 ± 4
1150	12.47 ± 0.08	90.9 ± 0.04	311 ± 2
1160	9.98 ± 0.2	86.7 ± 0.07	235 ± 3
1200	8.12 ± 0.15	81.2 ± 0.05	267 ± 2

The values were obtained from specimens sintered at different peak temperatures. All processes used a heating rate of 5 °C/min, and the specimen was held at the peak temperature for 10 min

4PH stainless steel powder, the optimal peak temperature is shown to be 1150 °C, which results in a greater sintered density and better mechanical properties. This increase in the relative density may be caused by the decrease in the number of pores within the material, and the decline in the relative density with a peak sintering temperature greater than 1150 °C may be caused by the non-uniformity of the grain growth within the material, which increases the material's open porosity [35].

3.1.2 Holding time

In the second tests, all samples were sintered to the same peak temperature of 1150 °C, which was the optimal peak temperature determined by the first tests. The durations of the holding time at the peak temperature were changed for each of these tests, while other processing factors were held constant to exclude the effects of other factors. Under this condition, the sintering results for different holding times are shown in Table 3.

The results shown in Table 3 indicate that an optimal heating duration exists for the peak temperature in MW-assisted sintering. With 17-4PH stainless steel powder, a holding time of 10 min is shown to produce the greatest density and best mechanical properties. With CRH sintering, an optimal holding duration also exists. Shorter holding times are shown to be insufficient for proper densification, while longer durations may lead to grain coarsening [30].

3.1.3 Heating rate

For the third group of the tests, the heating rates were varied. The optimal peak temperature (1150 °C) and holding time (10 min) identified earlier were used as the optimal values determined by two previous sets of tests. To investigate the effects of the heating rate in detail, the specimens were heated directly to the peak temperature from the ambient temperature and were held there for 10 min. The heating rates were set at different values in different tests, and the results of the MW-assisted sintering for different heating rates are shown in Table 4.

From the results in Table 4, a heating rate of 50 °C/min damaged the specimen; thus, a heating rate that is too high can produce an uneven temperature distribution within the material and can lead to the distortion or collapse of the material. A heating rate of 30 °C/min was shown to be optimal for the MW-assisted sintering of 17-4PH stainless steel. Based on reference [23], different shrinkage rates and different physical properties are the results of different porosities in MW-sintered samples. The porosity depends on the heating rate; thus, it is reasonable that the shrinkage, the relative density and the Vickers hardness also depend on the heating rate. At a heating rate of 30 °C/min during the MW-assisted sintering of 17-4PH stainless steel powders, the lowest porosity was obtained, resulting in a greater density and a greater hardness in the sintered specimens.

3.1.4 Pre-sintering temperature

Based on the above-mentioned results, specimens were heated to the peak temperature of 1150 °C at a heating rate of 30 °C/min and were then held at the peak temperature for 10 min. Then, the pre-sintering stage of the sintering process was analysed. Before the formal sintering stage, the specimens were heated to a pre-sintering temperature and then held for 30 min. The results for different pre-sintering temperatures are shown in Table 5. A test without pre-sintering was also performed for comparison with the other processes.

In Table 5, the best result was obtained by the process without the pre-sintering stage. If pre-sintering is necessary to obtain a given initial stiffness, a lower temperature should be used to produce a better quality material. The primary role of pre-sintering is to provide an initial stiffness for the initial stage of sintering. In some case, rapid heating induces inhomogeneities in the temperature; thus, the sintered specimen requires a given initial strength to prevent distortion or damage when sintering begins. Pre-sintering is thus unnecessary and provides no beneficial effect.

Table 3 Comparison of the shrinkages along the *x*-direction (Fig. 2), the relative densities and the Vickers hardnesses

Holding time (min)	Size shrinkage (%)	Relative density (%)	Vickers hardness (HV)
5	8.81 ± 0.3	85.9 ± 0.08	238 ± 1
10	12.47 ± 0.1	90.9 ± 0.03	311 ± 2
15	8.32 ± 0.25	84.6 ± 0.1	253 ± 2
20	8.19 ± 0.4	83.4 ± 0.14	277 ± 3

The values were obtained from the specimens sintered using MW with different holding times for the same peak temperature. All processes used a heating rate of 5 °C/min, and all specimens were sintered at the same peak temperature of 1150 °C

Table 4 Comparison of the shrinkages along the *x*-direction (Fig. 2), the relative densities and the Vickers hardnesses

Heating rate (°C/min)	Size shrinkage (%)	Relative density (%)	Vickers hardness (HV)
10	11.11 ± 0.33	92 ± 0.15	227 ± 2
20	15.15 ± 0.15	95 ± 0.08	299 ± 2
30	16.11 ± 0.07	96.6 ± 0.05	316 ± 1
40	14.90 ± 0.55	93.6 ± 0.20	231 ± 5
50	Specimen damaged		

The values were obtained from specimens sintered using MW at different heating rates. All processes sintered the material at the same peak temperature of 1150 °C, and the material was held at the peak temperature for 10 min

A conclusion can be drawn from the facts mentioned in Sect. 2: The optimal choice for the MW-assisted sintering process for a compacted specimen of 17-4PH stainless steel powder with a powder size near 11 μm is shown in Fig. 3.

3.2 Microstructure

Sintered metal injection moulding (MIM) parts are expected to have some residual porosity and typically have densities ranging from 95 to 99% of the theoretical density. A finer starting powder particle size is observed, in general, to result in finer pores.

The microstructures of the sintered materials in this study have been observed using optical microscope. The sintering stage was interrupted at different temperatures from 950 to 1150 °C and left to cool to allow observation of the corresponding microstructures. When the peak temperature was achieved, a holding time of 10 min was maintained. The evolution of the micrographs from powders to the sintered material is shown in Fig. 4a–f.

Figure 4 shows the evolution of the particle crystallization. When sintered to 950 °C, the material just began the sintering process. The samples are shown to be porous and be composed of small grains. As the sintering temperature increased, the number of pores decreased, and the rate of grain growth markedly increased. From Fig. 4d, f, marked grain growth is shown; most of the larger pores are located at the grain boundary. This phenomenon is favourable for the evacuation of gas entrapped in the porous powder compact and for the densification process. When the temperature reached 1150 °C (Fig. 4f), relatively larger pores that were not particularly uniformly distributed were nearly eliminated; this phenomenon relates well to the mechanical properties of the final samples.

Table 5 Comparison of the shrinkages along the *x*-direction (Fig. 2), the relative densities and the Vickers hardnesses

Pre-sintering temperature (°C)	Size shrinkage (%)	Relative density (%)	Vickers hardness (HV)
900	9.33 ± 0.45	83.7 ± 0.04	182 ± 2
600	10.12 ± 0.55	87.8 ± 0.13	190 ± 2
400	12.15 ± 0.35	89.9 ± 0.08	207 ± 3
270	13.94 ± 0.08	93.4 ± 0.10	274 ± 1
No pre-sintering stage	16.11 ± 0.10	96.6 ± 0.05	316 ± 2

The values were obtained from the specimen sintered using MW at different pre-sintering temperature. For all processes, the specimen was heated at the same heating rate of 30 °C/min up to the same peak temperature of 1150 °C and held at the peak temperature for 10 min

3.3 Distribution of the Vickers hardness

During MW processing, heat is produced inside the bulk material and sent out via radiation and convection from the outer surfaces of the specimens; thus, a thermal gradient occurs. During the MW heating of the sintering process, the temperature in the core is generally greater than the temperature on the surface. The outer surface at different positions on the specimen is, thus, subjected to different temperatures due to the irregular shape of the sintered body. The sintered material closer to the centroid becomes denser and generally exhibits better mechanical properties; this phenomenon can be demonstrated by detection of the hardness distribution over the polished cross section of the specimen.

The hardness distribution on a plane section was measured using a specialized procedure. A cross section near the middle plane of the specimen was prepared. On the polished section plane, nine small areas were arranged along the horizontal and vertical axes, as shown in the legend in the top right corner of Figs. 5 and 6. These areas were labelled in sequence from ×1 to ×5 and from y1 to y5. In each small area, five spots were tested. The average value of the five test results was recorded as the formal hardness of the small area.

As expected, the experimental results in Figs. 5 and 6 demonstrate the nature of MW-assisted sintering. The values at symmetrical positions (e.g., left and right or up and down) are shown to not be symmetric. The asymmetry in the values of the Vickers hardness was induced via hybrid MW-assisted sintering. For example, points y4 and y5 in the lower half were closer to the susceptor than points y2 and y1 in the upper half. Their closer location relative to the assisted heating SiC material resulted in greater heating rates and greater Vickers hardness values. It appears reasonable to claim that the contribution of the magnetic field is more important than the contribution of the electric field. However, the main contribution to the sample heating is due to the infrared radiation of the SiC susceptors. The SiC screens partially block the electromagnetic fields. The SiC susceptors play an auxiliary role in microwave heating. The physical properties of 17-4PH stainless steel powder are not sufficient to provide coupling with the electromagnetic field at a low temperature. The impact by

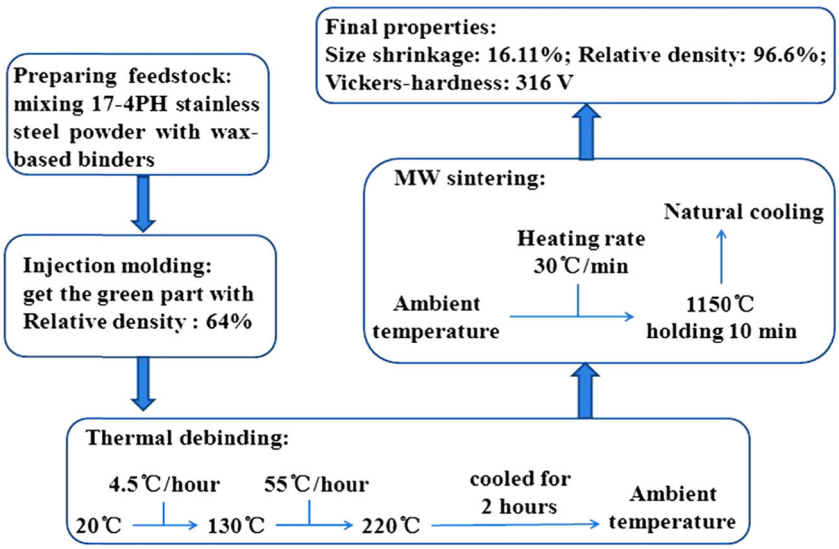

Fig. 3 Optimal process proposed for the MW-assisted sintering of specimens made of compacted 17-4PH stainless steel powder

microwave directly on the heating of the powder is very difficult due to the departure from a cold state. However, the property of powder compact can be altered by increasing the temperature. The effective heating of the test sample occurs

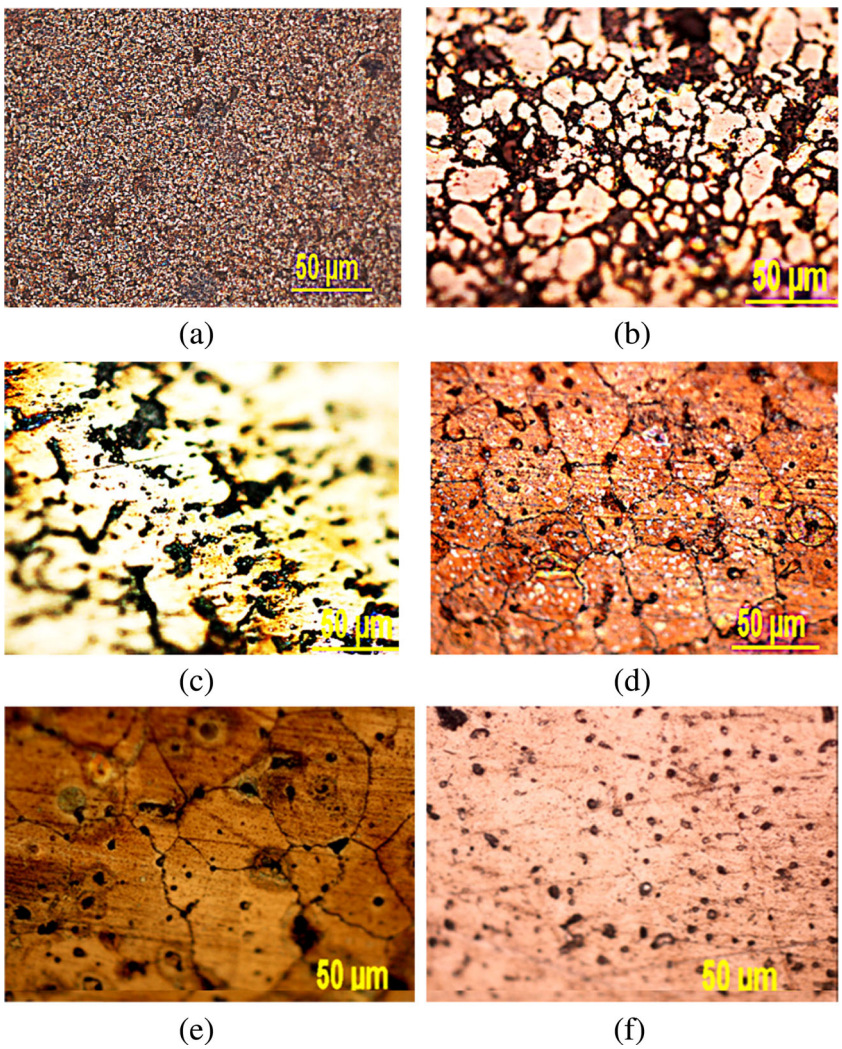

Fig. 4 Micrographs of the microstructure evolution for the MW-assisted sintering of the 17-4PH stainless steel powder observed using optical microscope: MW-assisted sintering at **a** 950 °C, **b** 1000 °C, **c** 1050 °C, **d** 1100 °C, **e** 1140 °C, **f** 1150 °C and held for 10 min

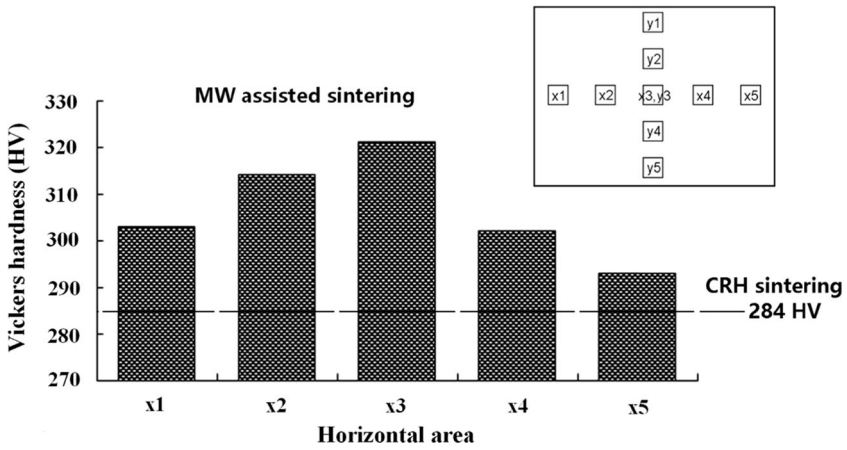

Fig. 5 Vickers hardness values for each small area along the horizontal direction

after the pre-heating or auxiliary heating using the SiC susceptors, when its properties become sufficient to provide a strong induction at a relatively higher temperature. Then, the effective heating is produced inside the powder impact for the true sintering process. As an auxiliary heating source, the SiC susceptors play another role to homogenize the temperature in the furnace cavity.

The difference in the hardness values among these small areas is approximately 20 to 30 Vickers units within such a small area. The gradient of the mechanical properties is also known to be significant in the sintered bodies; this phenomenon is caused by the rapid heating that occurs during the MW-assisted sintering due to the heat produced within the material. However, there is no available method that can slow the optimal heating rate; lower heating rates result in worse sintering qualities due to grain coarsening. This is an important fact that is demonstrated in the experimental results above. Thus, the gradient of the mechanical properties in the sintered bodies can be considered to be commonly produced by MW-assisted sintering and represents an important phenomenon to study the relationship between the evolution of the temperature gradient and the gradient of the mechanical properties in the sintered products. The prediction of gradient in the mechanical properties shows its potential value in studies of functionally graded materials. Further research on the modelling and simulation of these property gradients in MW-assisted sintering bodies should be performed.

None of the MW-sintered specimens in this study exhibited visually observable distortions. Because the shape of the studied specimens was not sensitive to distortion and because no precise measurement was applied to their geometries, this conclusion is just an estimate. The influence of the temperature gradient on the shape of the distortion of sintered bodies should be determined using specially designed specimens with precise measurement of their geometries.

3.4 Comparison with conventional sintering

3.4.1 Sintering of 17-4PH stainless steel using conventional sintering (CRH)

To study and compare the densification behaviours of the different sintering processes described in this study, the same debound components were sintered using CRH sintering in a

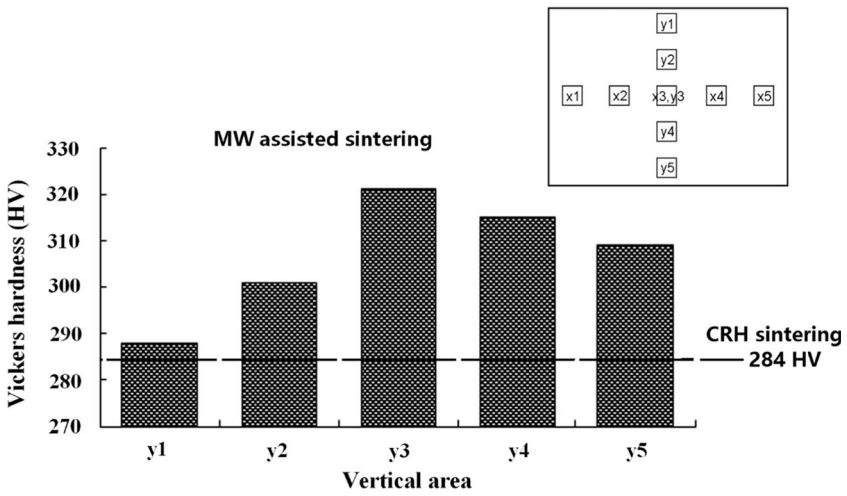

Fig. 6 Vickers hardness values for each small area along the vertical direction

vertical SETSYS® SETARAM evolution analyses. These specimens were heated to a peak temperature of 1350 °C at heating rates of 5, 10, 20 and 30 °C/min and then were held for 2 h. Based on the process proposed by Song [27], the temperature was held for 30 min when it reached 600 and 900 °C to ensure the homogenization of the temperature in the sintered bodies. The evolutions of the shrinkages and the shrinkage rates versus the temperature are shown in Fig. 7.

3.4.2 Comparison of MW and CRH sintering

Based on the conclusion results in Sect. 2.1.4, two tests were used for comparison. For the CRH sintering, the specimens were heated to 1350 °C at a heating rate of 5 °C/min and held at this temperature for 2 h. During the heating process, the temperature was held for 30 min when it reached 600 and 900 °C, respectively. For MW-assisted sintering, specimens were heated directly to 1150 °C at a heating rate of 30 °C/min and held at this temperature for 10 min. These test parameters were optimal, as determined above.

Table 6 shows the following: (1) The sintering of compacted 17-4PH stainless steel powder in an MW furnace reduces the required processing time by 90%; (2) the optimal peak temperature for the MW-assisted sintering is between 150 and 200 °C less than the optimal temperature for the CRH sintering; and (3) the achieved shrinkage, relative density and hardness of the MW-sintered materials are greater than the properties obtained using the CRH sintering according to a dilatometer. Similar results were obtained by Charmond [12], whose study showed that MW-sintered specimens in Y-tetragonal zirconia polycrystal powder exhibited a greater final density than the CRH-sintered specimens at the same temperature. A reasonable interpretation of the positive effect of the MW on the densification of the powder materials is the non-thermal effects of the microwaves, which are induced by high-frequency electromagnetic fields.

During a conventional sintering process, a high heating rate results in a thermal gradient within the compacts followed by a distortion and inhomogeneous microstructure in the sintered bodies. A slower heating rate was applied when using the isothermal holdings to achieve a stepwise variation of the temperatures. This represents a longer process time and greater cost and provides more cause for grain coarsening in the sintered compact. In microwave-assisted sintering, microwaves interact directly with the individual particles in powder compacts. This process provides rapid heating in a volumetric manner inside the sintered compact, which, therefore, restricts the generation of grain coarsening.

Compared to CRH sintering, MW-assisted sintering has different sintering mechanisms, such as the enhancement of the diffusion coefficient [36] and the eddy current for metals [37]. Therefore, it is reasonable that the peak temperature required for MW sintering is lower than for CRH sintering.

The final microstructures of the 17-4PH stainless steel sintered using CRH sintering and MW-assisted sintering with optimal process parameters are shown in Fig. 8a, b. The grain boundaries in both the conventional and microwave-sintered specimens are not obvious. It appears that the grains finally blend together, with some residual porosity inside. The MW-assisted sintering is fast with a high heating rate and resulted in a more homogeneous microstructure with lower porosities. In MW-assisted sintering for sintering a 17-4PH stainless steel, a final temperature of 1150 °C appears to result in the most homogeneous microstructure. This temperature results in the lowest pore fraction, smallest average pore size and most spherical pore shape in the specimen sintered using MW sintering, as seen in Fig. 8a, b. Compared to the specimen sintered using MW-assisted sintering, it is clear that many more and larger gas pores are present in the specimen sintered using CRH sintering; this phenomenon is caused by the heating characteristics of CRH sintering, where heat is conducted from the outer surface into the core of the specimen. This direction of heat conduction is opposite to the outward gas exhaust. The outer layer of the powder is, thus, easier to sinter and closes its pores earlier in the sintering process, and the outer layer obstructs the paths of gas exhausting from the

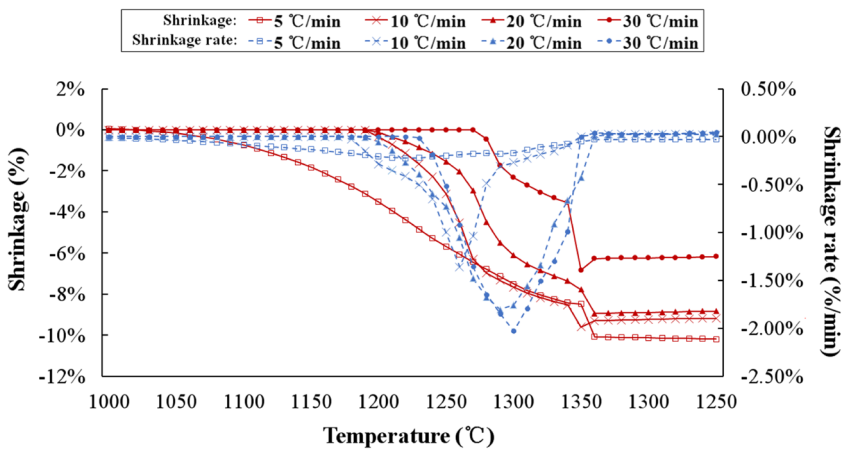

Fig. 7 Shrinkage and shrinkage rate versus temperature during the sintering of 17-4PH stainless steel powder specimens at different heating rates

Table 6 Comparison of the sintering time, peak temperature and final properties of the sintered specimens obtained using CRH and MW-assisted sintering

Sintering mode	Sintering time (min)	Peak temperature (°C)	Size shrinkage (%)	Relative density (%)	Vickers hardness (HV)
CRH	445	1350	14.95 ± 0.15	95.2 ± 0.08	284 ± 2
MW	48	1150	16.11 ± 0.10	96.6 ± 0.05	316 ± 2

inside the material. Some gas remains inside the specimen, which then forms large pores. Compacted powder heated by microwaves is more homogeneous in its microstructure, despite the high heating rate it experiences. This phenomenon, thus, exemplifies the advantage of volumetric heating provided by microwaves. This illustrates why specimens produced by MW-assisted sintering exhibit greater densities, a more homogeneous microstructure, better surface qualities and better mechanical properties.

3.4.3 Mechanical behaviours (Vickers hardness, ultimate tensile stress) of MW and CRH sintering and comparison with MPIF standard tests

High-strength metallic materials are typically very sensitive to small defects that locally give rise to stress concentrations. The comparison of mechanical behaviours of 17-4PH as a bulk and sintered material is described in Table 7. The influence of the mechanical properties on the initial particle size of the 17-4PH stainless steel sintered using CRH sintering at room temperature has been recently studied by Seerane et al. [40]. In our case, for the same mean size powders, the best hardness was obtained at 284 ± 2 HV, which corresponds to 95.2% of the relative density and is nearly equivalent to 280 HV and 97.5% of the relative density, which corresponds to the mechanical result by Seerane et al. [40]. Figure 9 summarizes the measured mechanical properties of the sintered parts and the respective as-sintered 17-4PH stainless steel minimum MPIF standard 35 specifications (MPIF, 2007). However, for a comparison of the Vickers hardness, using MW-assisted sintering, the minimum standard value has been obtained for all directions, as seen in Figs. 5 and 6. In the case of the best parameters, at position ×5, the high value corresponding to 320 ± 5 HV is largely superior compared to the standard MPIF value (280 ± 5 HV), as seen in Fig. 9a.

A correlation between the evolution of the hardness and the tensile strength is in agreement with the findings by Gulsoy et al. [41], and this relationship is also known to be common [42, 43]. The ultimate tensile stress value, using MW-assisted sintering, was approximately 940 MPa, as seen in Fig. 9b. This value is superior to the MPIF requirement [39] corresponding to a minimal value of 800 MPa.

The hardness and ultimate tensile stress compared to the standard MPIF values validate the 17-4PH material properties using the MIM and MW-assisted sintering process [40], as seen in Fig. 9a, b.

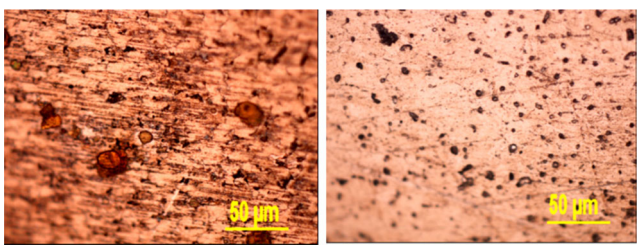

(a) CRH (b) MW assisted sintering

Fig. 8 Micrographs of the microstructures obtained from the specimens sintered using CRH sintering (**a**) and MW-assisted sintering (**b**)

4 Conclusions

Metal injection moulding of specimens using PM 17-4PH stainless steels was successfully consolidated to nearly full density using MW-assisted sintering. The experiments in this study were performed in a microwave laboratory system with a multi-mode cavity. The optimal heating cycle was determined from the experimental results, and the optimal result was obtained by heating directly from ambient temperature to 1150 °C at a heating rate of 30 °C/min and then holding the specimen at the peak temperature for 10 min. The specimen with the greatest density (96.6%) and best mechanical properties (Vickers hardness = 316 V, ultimate tensile stress = 940 MPa) was achieved using these optimal parameters. The sintered density obtained in this study was 96.6%, which is not high enough to be nearly full density. The measured mechanical properties of the sintered parts using the MW-assisted sintering and the respective as-sintered 17-4PH stainless steel minimum standard MPIF specifications [42]

Table 7 Comparison of the mechanical properties of the 17-4PH stainless steel at room temperature for the bulk and the sintered material

Tensile strength (MPa)	Yield strength (MPa)	Elongation (%)	Vickers hardness (kgf/mm^2)	Reference
1030	983	21	352	[38]
800			284	[39]

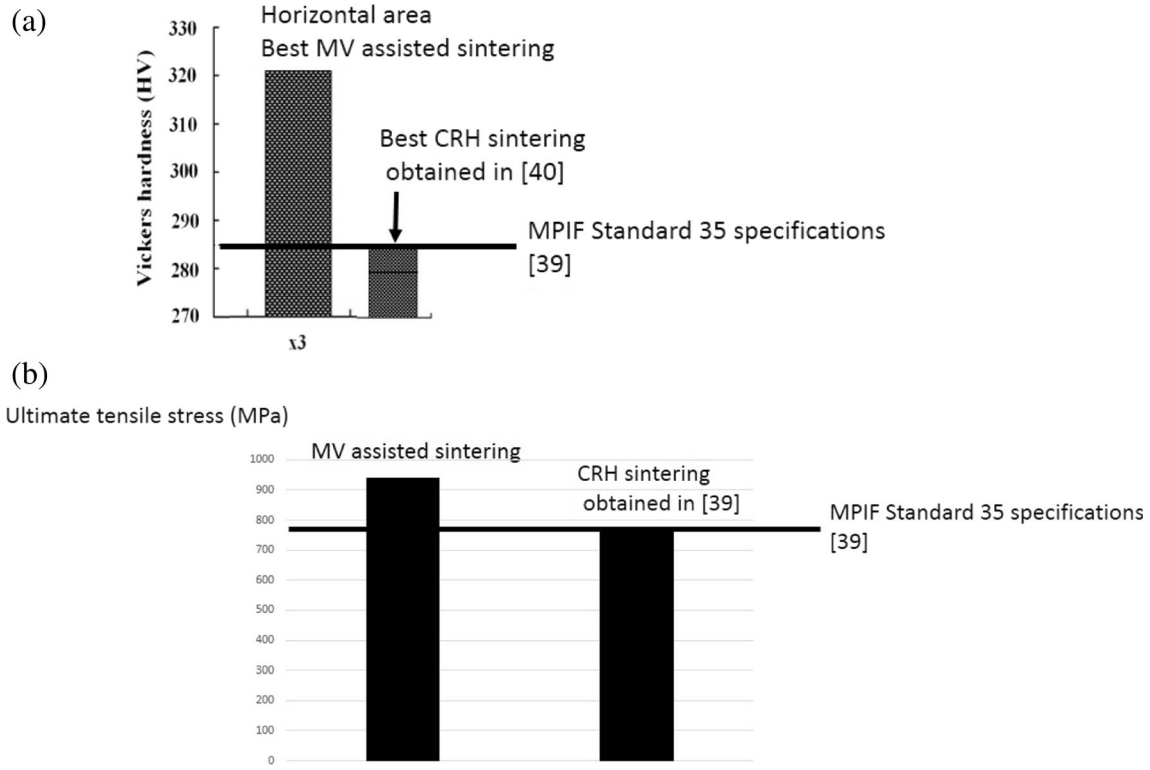

Fig. 9 The as-sintered MIM parts using CRH and MW-assisted sintering processes compared with MPIF standard 35 (Material Standard for a Metal Injection Moulded Part): **a** Vickers hardness and **b** the ultimate tensile stress

validate the PIM process and demonstrate the efficient and innovative MW sintering.

In this study, the results of observations and tests were different from results reported by Bose et al. [20]. The sintering of 17-4PH stainless steel powder using MW heating exhibited short processing times, requiring only 10% of the conventional sintering time to obtain better results, and lower peak temperatures (150 to 200 °C lower than the temperatures used in CRH sintering). Despite the high heating rates, the specimens did not show observable distortions or cracking, which demonstrates the important advantage of volumetric heating using MW. This illustrates why specimens produced using MW-assisted sintering also result in materials with a greater densification, a more homogeneous microstructure, better surface qualities and better mechanical properties. When a greater density is produced, sintering using MW heating also results in more shrinkage.

Sintering using MW heating also results in a marked gradient in the mechanical properties of the sintered material; this phenomenon is induced by the rapid internal heating and the other physical effects that are induced by microwaves. Studies of this phenomenon should continue to define and describe the applications of MW-assisted sintering products.

Microwave-assisted sintering generally results in fast sintering and more homogeneous microstructures. Evidently, this explanation is not complete. More complicated physical phenomena are still being studied to provide precise explanations. Additionally, modelling and simulating the generation of the gradient properties appear to be significant for future studies.

Acknowledgements This work was financially supported by the National Natural Science Foundation of China (Grant No. 11502219) and the Doctoral Research Foundation of Southwest University of Science and Technology (Grant No. 14zx7139). The authors also wish to thank the Femto-ST Institute for the experimental and simulation support.

Glossary MW, microwave; CRH, conventional resistive heating

References

1. Slaby SA, Kraft O, Eberl C (2016) Fatigue properties of conventionally manufactured and micro-powder-injection moulded 17-4 PH micro-components. Fatigue & Fracture of Engineering Materials & Structures 39:649–789
2. Ye H, Liu XY, Hong H (2008) Sintering of 17-4PH stainless steel feedstock for metal injection molding. Mater Lett 62:3334–3336
3. Sung HJ, Ha TK, Ahn S, Chang YW (2002) Powder injection moulding of a 17-4PH stainless steel and the effect of sintering temperature on its microstructure and mechanical properties. J Mater Process Techno 130-131:321–327
4. Jeefferie AR, Nurhashima S, Yuhazri MY, Sihombing H, Shukor SM, Abdullah NS, Omar MA (2011) Characterization of injection molded 17-4PH stainless steel prepared with waste rubber binder. Journal of Mechanical Engineering and Technology 3:11–21

5. Mutlu I, Oktay E (2011) Processing and properties of highly porous 17-4 PH stainless steel. Powder Metallurgy and Metal Ceramics 50:73–82
6. Suri P, Smarslok BP, German RM (2006) Impact properties of sintered and wrought 17-4 PH stainless steel. Powder Metall 49:40–47
7. Simchi A, Rota A, Imgrund P (2006) An investigation on the sintering behavior of 316L and 17-4PH stainless steel powders for graded composites. Mater Sci Eng A 424:282–289
8. Imgrund P, Rota A, Simchi A (2008) Microinjection moulding of 316L/17-4PH and 316L/Fe powders for fabrication of magnetic-nonmagnetic bimetals. J Mater Process Technol 200:259–264
9. Campañone LA, Paola CA, Mascheroni RH (2012) Modeling and simulation of microwave heating of foods under different process schedules. Food Bioprocess Technol 5:738–749
10. Menezes RR, Souto PM, Kiminami RHGA (2007) Microwave hybrid fast sintering of porcelain bodies. J Mater Process Technol 190: 223–229
11. Leonelli C, Veronesi P, Denti L, Gatto A, Iuliano L (2008) Microwave assisted sintering of green metal parts. J Mater Process Technol 205:489–496
12. Charmond S, Carry CP, Bouvard D (2010) Densification and microstructure evolution of Y-tetragonal zirconia polycrystal powder during direct and hybrid microwave sintering in a single-mode cavity. J Eur Ceram Soc 30:1211–1221
13. Wu Q, Zhang X, Wu B, Huang W (2013) Effects of microwave sintering on the properties of porous hydroxyapatite scaffolds. Ceram Int 39:2389–2395
14. Chockalingam S, Earl DA (2010) Microwave sintering of Si3N4 with $LiYO_2$ and ZrO_2 as sintering additives. Mater Des 31:1559–1562
15. Chockalingam S, Traver HK (2010) Microwave sintering of β-SiAlON-ZrO2 composites. Mater Des 31:3641–3646
16. Bykov Y, Egorov S, Eremeev A, Kholoptsev V, Plotnikov I, Rybakov K, Semenov V, Sorokin A (2010) Effects of microwave heating in nanostructured ceramic materials. Powder Metallurgy and Metal Ceramics. 49:31–41
17. Chandrasekaran S, Basak T, Ramanathan S (2011) Experimental and theoretical investigation on microwave melting of metals. J Mater Process Technol 211:482–487
18. Srinath MS, Sharma AK, Kumar P (2011) A new approach to joining of bulk copper using microwave energy. Mater Des 32: 2685–2694
19. Panda SS, Singh V, Upadhyaya A, Agrawal D (2006) Sintering response of austenitic (316L) and ferritic (434L) stainless steel consolidated in conventional and microwave furnaces. Scr Mater 54: 2179–2183
20. Bose A, Agrawal D, Dowding RJ (2004) Preliminary investigations into microwave processing of powder injection molded 17-4 PH stainless steel. International Conference on Powder Metallurgy and Particulate Materials 53
21. Quinard C, Song J, Barriere T, Gelin JC (2011) Elaboration of PIM feedstocks with 316L fine stainless steel powders for the processing of micro-components. Powder Technol 208:383–389
22. Mariappan R, Kumaran S, Rao TS (2009) Effect of sintering atmosphere on structure and properties of austeno-ferritic stainless steels. Mater Sci Eng A 517:328–333
23. Oliveira FAC, Marcelo T, Alves C, Santos M, Mascarenhas J, Trindade B (2014) Effect of particle size of starting oxide powders on the performance of doped-lanthanum oxyapatite produced by mechanical alloying followed by microwave sintering. Adv Powder Technol 25: 1455–1461
24. Ertugrul O, Park H-S, Onel K, Willert-Porada M (2014) Effect of particle size and heating rate in microwave sintering of 316L stainless steel. Powder Technol 253:703–709
25. Shi JJ, Cheng Z, Gelin JC, Barriere T, Liu B Multi-physic coupling and full cycle simulation of microwave sintering, The Advances in Materials and Processing Technologies, AMPT 2015 Conference, December 14–17 2015, Madrid, Spain, In Symposium: New Trends in Powder Metallurgy, 1–6
26. Shi JJ (2014) Experiment and simulation of micro-injection molding and microwave sintering, [Co-tutorial PhD Thesis]: Chengdu&Besancon: Southwest Jiaotong University & Franche-Comte University
27. Song J, Gelin JC, Barriere T, Liu B (2006) Experiments and numerical modelling of solid state sintering for 316L stainless steel components. J Mater Process Technol 177:352–355
28. Yang RB, Liang WF, Lou CW, Lin JH (2012) Electromagnetic and microwave absorption properties of magnetic stainless steel powder in 2-18 GHz. J Appl Phys 111:07A338
29. Bahadoor A, Wang Y, Afsar MN (2005) Complex permittivity and permeability of barium and strontium ferrite powders in X, KU, and K-band frequency ranges. J Appl Phys 97:105–107
30. Kong X, Barriere T, Gelin JC (2012) Determination of critical and optimal powder loadings for 316L fine stainless steel feedstocks for micro-powder injection molding. J Mater Process Technol 212: 2173–2182
31. Quinard C, Barriere T, Gelin JC (2009) Development and property identification of 316L stainless steel feedstock for PIM and μPIM. Powder Technol 190:123–128
32. Enneti RK, Shivashankar TS, Park SJ, German RM, Atre SV (2012) Master debinding curves for solvent extraction of binders in powder injection molding. Powder Technol 228:14–17
33. Nayer A (1997) The metals data book. McGraw-Hill, New York (NY)
34. Kim-Hak O, Soulier M, Szkutnik PD, Saunier S, Simon J, Goeuriot D (2012) Microwave sintering and thermoelectric properties of p-type $(Bi0.2Sb0.8)_2Te_3$ powder. Powder Technol 226:231–234
35. Chen YC, You HM (2015) Effect of sintering temperature on microstructures and microwave dielectric properties of Zn_2SnO_4 ceramics. Mater Chem Phys 154:94–99
36. Ma J, Diehl JF, Johnson EJ, Martin KR, Miskovsky NM, Smith CT, Weisel GJ, Weiss BL, Zimmerman DT (2007) Systematic study of microwave absorption, heating, and microstructure evolution of porous copper powder metal compacts. J Appl Phys 101:074906
37. Yoshikawa N (2010) Fundamentals and applications of microwave heating of metals. The Journal of Microwave Power and Electromagnetic Energy 44:4–13
38. Schönbauer BM, Yanase K, Endo M (2017) The influence of various types of small defects on the fatigue limit of precipitationhardened 17–4PH stainless steel. TheorAppl FractMech 87: 35–49
39. MPIF (2016) Materials standard for metal injection molded parts, MPIF standard 35. Metal Powder Industries Federation, Princeton, pp 19–19
40. Seerane M, Ndlangamandla P, Machaka R (2016) The influence of particle size distribution on the properties of metal injectionmoulded 17-4 PH stainless steel. J of the Southern Africa Institute of Mining and Metallurgy 116:935–940
41. Gulsoy HO, Ozgun O, Bilketay S (2016) A powder injection molding of Stellite 6 powder: sintering, microstructural and mechanical properties. Mater Sci Eng A 651:914–924
42. Gasko M, Rosenberg G (2011) Correlation between hardness and tensile properties in ultra-high strength dual phase steels.Mater Eng 18:155–159
43. Shen Y, Chawla N (2001) On the correlation between hardness and tensile strength in particle reinforced metal matrix composites. Mater Sci Eng A 297:44–47